Physics cross sections and event generation of e^+e^- annihilations at the CEPC *

Xin Mo(莫欣)[1;1)] Gang Li(李刚)[1;2)] Man-Qi Ruan(阮曼奇)[1)] Xin-Chou Lou(娄辛丑)[1,2]

[1] Institute of High Energy Physics, Chinese Academy of Sciences, Beijing 100049, China
[2] University of Texas at Dallas, Richardson, TX 75080-3021, USA

Abstract: The cross sections of the Higgs production and the corresponding backgrounds of e^+e^- annihilations at the CEPC (Circular Electron and Positron Collider) are calculated by a Monte-Carlo method, and the beamstrahlung effect at the CEPC is carefully investigated. The numerical results and the expected number of events for the CEPC are provided.

Keywords: CEPC, Higgs physics, cross section, Monte-Carlo generation

PACS: 13.66.Fg, 14.80.Bn, 07.05.-t **DOI:** 10.1088/1674-1137/40/3/033001

1 Introduction

The discovery of the Higgs boson [1,2] is a great milestone for modern particle physics. No matter whether it is the Standard Model (SM) Higgs or an indication of new physics, the discovery makes the Higgs mechanism more credible. Furthermore, precision measurements of the properties of the new Higgs boson are critical for Higgs physics; any deviation away from the SM expectation will improve our knowledge of the elementary particles and their interactions. With this consideration, an e^+e^- collider with high luminosity and energy is best suited for Higgs research.

The Circular Electron-Positron Collider (CEPC) [3] is a proposed circular collider. It is designed to run around 240−250 GeV and will deliver 5 ab^{-1} of integrated luminosity during 10 years of operation. About 10^6 Higgs events will be produced in a clean environment, which allows the measurement of the cross section of Higgs production as well as its mass, decay width and branching ratios with precision much better than those of hadron colliders.

Besides Higgs events, there will be a large number of electroweak processes generated at the CEPC, via the vector bosons W and Z. High electroweak statistics is essential for understanding the detectors precisely, for the precision measurements of Higgs properties. Moreover, these electroweak events can also be used to perform high precision measurements of the SM parameters, such as the forward-backward charge asymmetry ($A_{\rm FB}$).

The calculations in this paper are done with the WHIZARD generator [4, 5], which is one of the most popular Monte-Carlo generators for Higgs studies and is used by the International Linear Collider (ILC) [6–10] and Compact Linear Collider (CLIC) [11, 12] groups.

In this paper, we will investigate the physics cross sections and describe event generation at the CEPC. In Sec. 2, Higgs production is studied and the cross sections are given. The radiative correction to the cross sections is discussed in Sec. 3. In Sec. 4, the backgrounds of various final states are presented. Finally, a brief summary is provided in the Sec. 5.

2 Higgs production cross section

Due to the fact that the Higgs boson coupling

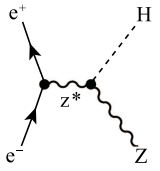

Fig. 1. Feynman diagram of the Higgsstrahlung process.

Received 9 June 2015, Revised 27 September 2015

∗ Supported by CAS/SAFEA International Partnership Program for Creative Research Teams, and funding from CAS and IHEP for the Thousand Talent and Hundred Talent programs, as well as grants from the State Key Laboratory of Nuclear Electronics and Particle Detectors

1) E-mail: moxin@ihep.ac.cn

2) E-mail: li.gang@ihep.ac.cn

to fermions is proportional to the fermion mass, the process $e^+e^- \to H$ is highly suppressed. The dominant Higgs production in electron positron annihilation is the so-called Higgsstrahlung, an s-channel process in which a Higgs is produced in association with a Z boson, as shown in Fig. 1.

The other two typical t-channel processes, the vector boson fusions, as shown in Fig. 2, are sizable contributions to the Higgs production that will increase with the center of mass energy.

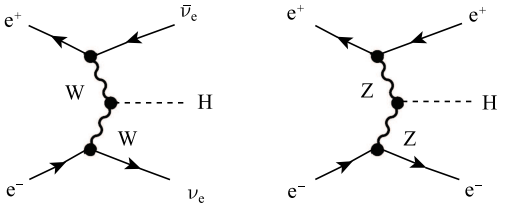

Fig. 2. Feynman diagrams of vector boson fusions.

The cross section of the Higgsstrahlung process can be written as

$$\sigma(e^+e^- \to ZH) = \frac{G_F^2 m_Z^4}{96\pi s}(v_e^2+a_e^2)\lambda^{\frac{1}{2}}\frac{\lambda+12m_Z^2/s}{(1-m_Z^2/s)^2}. \quad (1)$$

The cross section for vector fusion production can be written in a similar compact form as [13]

$$\sigma(e^+e^- \to VV \to l\bar{l}H) = \frac{G_F^3 m_V^4}{4\sqrt{2}\pi^3}\int_{x_H}^1 dx \int_x^1 \frac{dyF(x,y)}{[1+(y-x)/x_V^2]^2}, \quad (2)$$

$$F(x,y) = \left(\frac{2x}{y^3}-\frac{3x+1}{y^2}+\frac{x+2}{y}-1\right)\left[\frac{z}{z+1}-\log(z+1)\right] + \frac{xz^2(1-y)}{y^3(z+1)},$$

where V stands for the vector bosons Z or W, and the dimensionless variables are defined as

$$x_H = m_H^2/s, \quad x_V = m_V^2/s \quad z = y(x-x_H)/(xx_V).$$

For moderate Higgs masses and energies, the cross sections of vector boson fusion are suppressed compared with Higgsstrahlung due to the additional electroweak couplings. With increasing energy, the cross sections of VBF processes rise logarithmically as the typical t-channel process [14]

$$\sigma(e^+e^- \to VV \to l\bar{l}H) \approx \frac{G_F^3 m_V^4}{4\sqrt{2}\pi^3}\log\frac{s}{m_H^2}. \quad (3)$$

Meanwhile, the cross section of Higgsstrahlung decreases asymptotically according to the scaling law $\sim g_F^4/s$. Therefore, vector boson fusion will become the dominant contribution to the Higgs production far beyond the ZH threshold.

The Higgsstrahlung, WW and ZZ fusions are shown in Fig. 3. Above the ZH threshold, the cross section of Higgsstrahlung rises rapidly and reaches its maximum around 250 GeV. The dashed curves represent the cross sections without the ISR effect, which will be discussed in the following section.

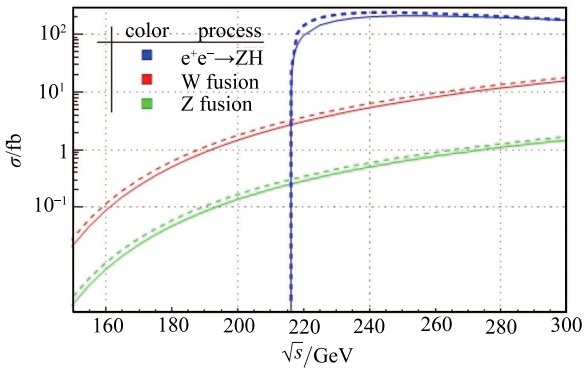

Fig. 3. (color online) The cross sections of various Higgs productions, in which the solid lines are with ISR correction and the dashed ones are without.

3 Initial state radiation and beamstrahlung

Initial state radiation (ISR) is an important issue in high energy processes, especially for lepton colliders. ISR affects cross section significantly, for example, reducing the ZH cross section by more than 10% within the WHIZARD framework as shown in Fig. [3]. Though the cancellation for soft and collinear photons has been validated to all orders in perturbation theory [15], and hard photon emission can in principle also be calculated perturbatively order by order in QED [16,17], the maximal order for the hard photon is set to be 3 in the calculation.

Table 1. Comparison of cross sections with beamstrahlung turned on and off.

	ISR/fb	ISR & Beamstrahlung/fb
$\sigma(e^+e^- \to ZH)$	212	211
$\sigma(e^+e^- \to \nu\bar{\nu}H)$	6.72	6.72
$\sigma(e^+e^- \to e^+e^-H)$	0.63	0.63
$\sigma(e^+e^- \to q\bar{q})$	50216	50416
$\sigma(e^+e^- \to W^+W^-)$	15484	15440
$\sigma(e^+e^- \to ZZ)$	1033	1030

Besides ISR, another macro effect at high luminosity electron-positron colliders, beamstrahlung, also affects the cross section. In the storage ring the beamstrahlung effect makes the beam energy spread larger

and reduces the center of mass energy [18]. A tool that is widely used to simulate this effect for e^+e^- colliders is GuineaPig++ [19,20]. The total energy spread caused by beamstrahlung and synchrotron radiation is studied by Monte-Carlo simulation and determined to be 0.1629% at CEPC [18]. In the event generation, even though the energy spread is taken into account, the corrections to the cross sections of Higgs production are negligible while the observable difference in $e^+e^- \to q\bar{q}$ is only at percentage level. The results are listed in Table 1.

4 Cross sections of backgrounds

4.1 Two-fermion backgrounds

Two-fermion final states are the major backgrounds in electron positron colliders. The leading process is quark pair production and the cross section is around 50 pb at $\sqrt{s} \sim 250$ GeV. Another important two-fermion process is di-muon production, whose cross section reaches 5 pb. The cross sections of these two processes are shown in Fig. 4, and the expected numbers of $q\bar{q}$ and $\mu^+\mu^-$ events at 250 GeV are around 250×10^6 and 22×10^6, respectively (see Table. 4), for the CEPC program.

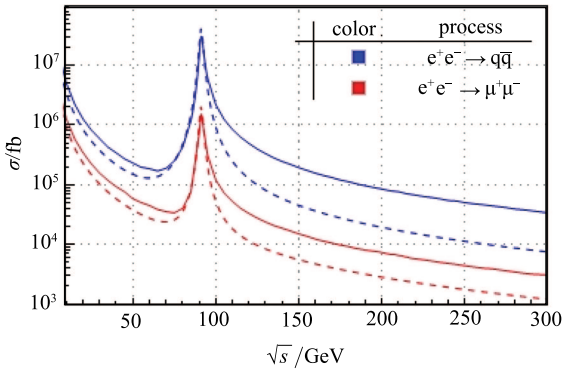

Fig. 4. (color online) The cross sections of $e^+e^- \to q\bar{q}$ and $\mu^+\mu^-$ processes, in which the solid (dashed) lines are with(without) ISR correction.

The cross sections are much higher in the vicinity of the Z pole, and the precision of Z pole measurement could benefit from such large statistics. For the partial decay width $Z \to \mu^+\mu^-$, the statistical uncertainty can be reduced to 0.03% [3] compared to 0.15% for LEP experiments [21–24]. The electroweak mixing angle is an important free parameter in the SM, rotating the original $SU(2)\times U(1)$ field into the physically observed vector boson state. It is sensitive to higher-order electroweak corrections and could be a precise test of SM perturbative theory. The precision of the mixing angle is expected to be 0.02% from the $Z \to b\bar{b}$ process [3]. The precision measurement of the mass of the Z boson may also be improved at CEPC, and the statistical uncertainty is expected to be 0.1 MeV [3].

Both the measurements of the electroweak mixing angle and the mass of the Z boson need the data from a Z pole run as well as off-peak runs. A preliminary data taking plan for Z pole physics was proposed in [3], and the luminosities as well as cross sections at different energy points are listed in Table 2. Of course, this scan scheme would be optimized in future studies.

Table 2. A possible scan scheme around the Z pole at CEPC.

$\sqrt{s}$/GeV	88.2	89.2	90.2	91.1876
$\int L/\mathrm{fb}^{-1}$	10	10	10	100
$\sigma(e^+e^- \to q\bar{q})$/nb	4.22	7.92	17.22	30.20
$\sigma(e^+e^- \to \mu\mu)$/nb	0.22	0.41	0.87	1.51
$\sqrt{s}$/GeV	92.2	93.2	94.2	
$\int L/\mathrm{fb}^{-1}$	10	10	10	
$\sigma(e^+e^- \to q\bar{q})$/nb	22.24	12.78	8.18	
$\sigma(e^+e^- \to \mu\mu)$/nb	1.11	0.65	0.42	

4.2 Bhabha scattering

The small-angle (SABH) and large-angle (LABH) Bhabha scattering processes both play important roles in e^+e^- collider physics. SABH is mainly used to measure the instant luminosity of the accelerator due to the huge cross section, while LABH can be used as a cross check of the luminosity measurement of the SABH for the calibration of the detector during the offline stage.

The observed cross section of SABH in the next-to-leading order for theoretical prediction depends not only on the angular range covered by the detector, but also on the cut of the electron energy. Although WHIZARD is designed to calculate it up to next leading order, unfortunately, it is not adequate for the SABH process, especially in the low energy region, as shown in Fig. 5.

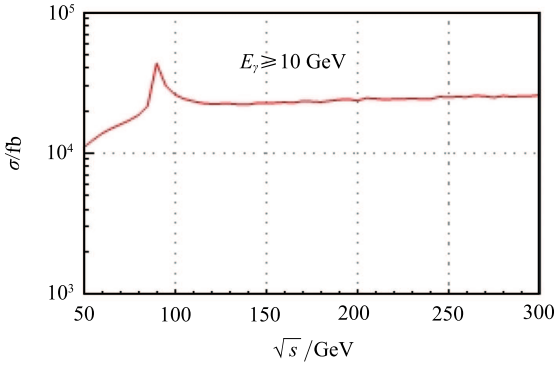

Fig. 5. (color online) The cross section of Bhabha scattering, with ISR included and a cut for photon energy applied.

4.3 Vector boson pair production

The electroweak processes for vector boson pair production are $e^+e^- \to W^+W^-$ and $e^+e^- \to ZZ$. The cross sections of on-shell production for vector bosons are plotted in Fig. 6. The s-channel process provides the dominant contribution in the CEPC energy region.

Vector boson pair production is crucial for the precision measurement of the Higgs. For example, W bosons can be produced via Fig.7, and they can decay further into a quark-antiquark pair, i.e., $W^+W^- \to u\bar{u}d\bar{d}$ or $c\bar{c}s\bar{s}$, which creates four jets and tends to contaminate the ZH in many cases. Although ZZ pair production is one order of magnitude smaller than WW, it is especially severe as a background for Higgs measurements as it may lead to the same final states and kinematics as ZH.

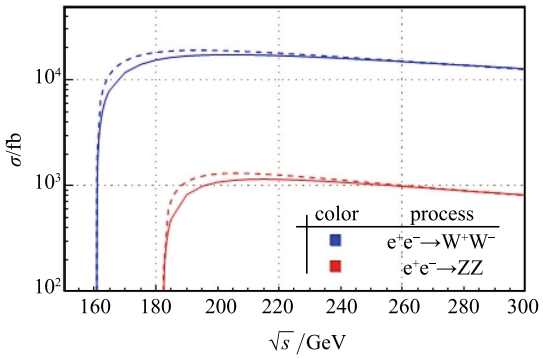

Fig. 6. (color online) The cross sections of $e^+e^- \to W^+W^-$ and ZZ processes, in which the solid lines are with ISR correction and the dashed ones without.

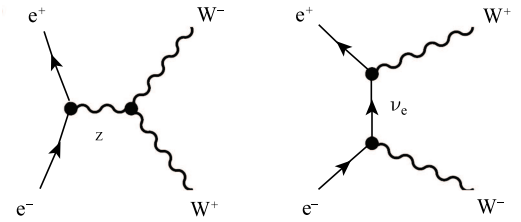

Fig. 7. Feynman diagrams for WW pair production.

Precision measurements of the W boson mass can be achieved by both the direct method and by threshold scan. By applying the direct method, the measurements can be performed with the same run at $\sqrt{s} = 250$ GeV, where most attention is paid to the Higgs. The main challenge of the direct method is the calibration of the detectors and the modeling of resolution, which is proportional to $\sqrt{s}$. Thanks to the high luminosity of CEPC, the uncertainty due to beamstrahlung can be reduced to ~ 1 MeV.

Besides the W boson mass measurements, these vector boson productions, W^+W^- and ZZ, are also a good resource for precision measurements of triple boson coupling in electroweak theory. Any deviation from the SM will be a hint for new physics beyond the Standard Model.

5 Classification of event samples

The Monte-Carlo samples generated for CEPC can be grouped into signal and background parts intuitively. The signal part includes all the Higgs production processes, both Higgsstrahlung and fusion. The backgrounds can be classified according to the final states. The final states with two fermions and four fermions contribute the most background for CEPC, since the center of mass energy of CEPC is not high enough for more particles in the final state.

Table 3. Number of Feynman diagrams for WW type processes.

	$u\bar{d}$	$c\bar{s}$	$\bar{e}\nu_e$	$\bar{\mu}\nu_\mu$	$\bar{\tau}\nu_\tau$
$d\bar{u}$	*43*	**11**	20	**10**	**10**
$s\bar{c}$	**11**	*44*	20	**10**	**10**
$e\bar{\nu}_e$	20	20	*56*	18	18
$\mu\bar{\nu}_\mu$	**10**	**10**	18	*19*	**9**
$\tau\bar{\nu}_\tau$	**10**	**10**	18	**9**	*20*

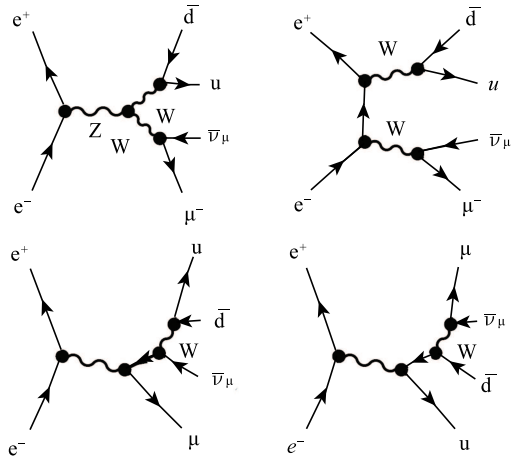

Fig. 8. Typical topologies of four-fermion production of WW type.

The classification scheme for four-fermion production, which is borrowed from LEP [25], depends crucially on the final state. The four fermions can be classified into two classes. The first class comprises the (up, anti-down or $l\bar{\nu}$) and (down anti-up or $\bar{l}\nu$) combinations,

$$(U_i \quad \bar{D}_i) + (\bar{U}_j \quad D_j),$$

which are produced by a virtual WW pair, named the "WW" process. The other class is the production of two fermion-antifermion pairs,

$$(f_i \quad \bar{f}_i) + (\bar{f}_j \quad f_j),$$

which is produced by two virtual neutral vector bosons, named the "ZZ" process.

A further restriction can be applied to these two types. If there is $e^{\pm}$ together with its neutrino and an on-shell W boson in the final state, this type is named the "Single W" process; Meanwhile, if there is an electron-positron pair and an on-shell Z boson in the final state, this case is named the "Single Z". Some final states consist of two mutually charge-conjugated fermion pairs, which could be from both virtual WW or ZZ; this type is called the "mixed type".

The typical structure of Feynman diagrams for the WW type is listed in Fig. 8; the final states could be produced through an intermediate W pair or W boson radiation. Further, the actual number of the Feynman diagrams is listed in Table. 3. The numbers in **bold** font are the general WW processes, which means there are two pairs of fermions in the final state without identical particles. The ordinary font and *italic* font describe the single W and mixed processes, respectively. The ZZ type has a similar structure to the WW type, and Ref. [25] is a good reference for details.

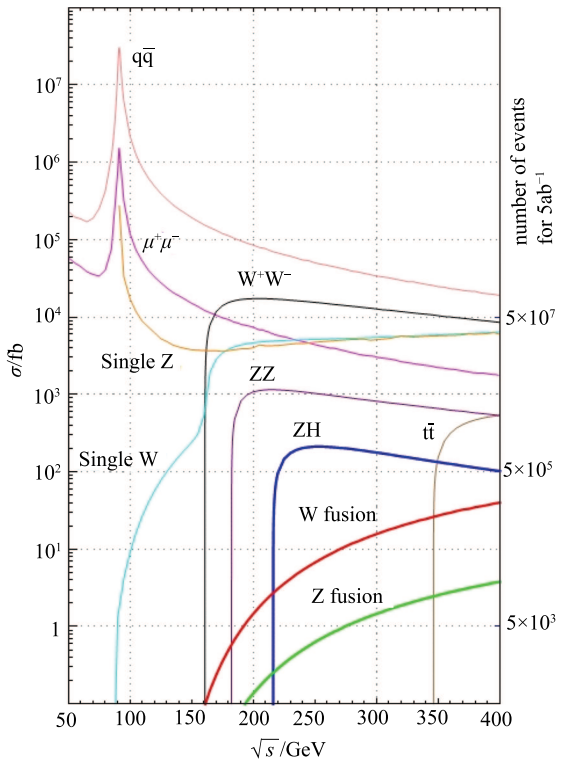

Fig. 9. (color online) The cross sections of major SM processes with ISR effect taken into account.

6 Summary

In summary, the cross sections of major Standard Model processes, including Higgs production as well as the major backgrounds, are plotted in Fig. 9, where the ISR effect has been taken into account.

In addition, the numerical results of these processes are listed in Table 4, as well as the expected number of events for a total luminosity of 5 ab^{-1} for a 10-year run. Based on the cross sections, the Monte-Carlo samples for Higgs analysis at CEPC have been generated by WHIZARD.

Table 4. Cross sections and numbers of events expected at 250 GeV for CEPC.

process	cross section	No. of events in 5 ab^{-1}
higgs production cross section in fb		
$e^+e^- \to ZH$	212	1.06×10^6
$e^+e^- \to \nu\bar{\nu}H$	6.27	3.36×10^4
$e^+e^- \to e^+e^-H$	0.63	3.15×10^3
total	219	1.10×10^6
background cross sections in pb		
$e^+e^- \to e^+e^-$	25.1	1.3×10^8
$e^+e^- \to qq$	50.2	2.5×10^8
$e^+e^- \to \mu\mu$ (or $\tau\tau$)	4.40	2.2×10^7
$e^+e^- \to WW$	15.4	7.7×10^7
$e^+e^- \to ZZ$	1.03	5.2×10^6
$e^+e^- \to eeZ$	4.73	2.4×10^7
$e^+e^- \to e\nu W$	5.14	2.6×10^7

In this paper, the cross sections of Higgs production and the background processes at the CEPC have been evaluated and the classification of the MC samples discussed. Most of the processes have been well calculated by WHIZARD. Bhabha processes should be studied more carefully in the future.

It is worth noting that there are several differences compared with previous studies for the ILC. First, CEPC and ILC have completely different environments. The beamstrahlung effect is much weaker (typically 2 orders of magnitude) at the CEPC, which leads to a negligible correction to the CEPC energy spread. Second, although 250 GeV has been investigated for our physics interests in this paper, the methods and tools could also be used at various other energy points, for example 240 GeV, at which the physics interests and project concerns could both be satisfied. Additionally, the SM backgrounds have been investigated more carefully than for the ILC project. All these prospects have been investigated for the CEPC in this paper.

References

1 G. Aad et al(ATLAS Collaboration), Phys. Lett. B, **716**: 1, (2012)
2 S. Chatrchyan et al(CMS Collaboration), Phys. Lett. B, **716**: 30, (2012)
3 M. Ahmad et al(The CEPC-SPPC Study Group), CEPC-SppC Preliminary Conceptual Design Report: Physics and Detector, http://cepc.ihep.ac.cn/preCDR/main_preCDR.pdf, retrieved 4th May 2015
4 W. Kilian, T. Ohl, and J. Reuter, Eur. Phys. J. C, **71**:1742, (2011)
5 M. Moretti, T. Ohl, and J. Reuter, arXiv: hepph/0102195
6 T. Behnke, J. Brau, B. Foster et al, arXiv:1306.6327
7 H. Baer, T. Barklow, K. Fujii et al, arXiv:1306.6352
8 C. Adolphsen, M. Barone, B. Barish et al, arXiv:1306.6353
9 C. Adolphsen, M. Barone, and B. Barish, arXiv:1306.6328
10 T. Behnke, J. Brau, and P. Burrows, Volum 4, arXiv:1306.6329
11 P. Lebrun, L. Linssen, A. Lucaci-Timoce et al, arXiv:1209.2543
12 L. Linssen, A. Miyamoto, M. Stanitzki et al, arXiv:1202.5940
13 M. Baillargeon, Production of a Higgs with Two Gauge Bosons, in e^+e^- Collisions at 500 GeV: The Physics Potential, in Proceedings of the Workshop Munich-Annecy-Hamburg, edited by P.M. Zerwas
14 W. Kilian, M. Kramer, and P. M. Zerwas, Phys. Lett. B, **373**:135, (1996)
15 V. N. Gribov and L. N. Lipatov, Sov. J. Nucl. Phys., **15**:675, (1972)
16 E. A. Kuraev and V. S. Fadin, Sov. J. Nucl. Phys., **41**:466, (1985)
17 M. Skrzypek and S. Jadach, Z. Phys. C, **49**:577, (1991)
18 http://cepc.ihep.ac.cn/preCDR/Pre-CDR_final_20150317.pdf, retrieved 17th March 2015
19 D. Schulte, CERN-PS-99-014-LP
20 D. Schulte, M. Alabau, P. Bambade, O. Dadoun, G. Le Meur, C. Rimbault, and F. Touze, Conf. Proc. C, **070625**: 2728, (2007)
21 A. Heister et al (ALEPH Collaboration), Eur. Phys. J. C, **22**:201, (2001)
22 G. Abbiendi et al (OPAL Collaboration), Phys. Lett. B, **546**:29, (2002)
23 J. Abdallah et al (DELPHI Collaboration), Eur. Phys. J. C, **40**:1, (2005)
24 M. Acciarri et al (L3 Collaboration), Phys. Lett. B, **448**: 152, (1999)
25 D. Bardina, M. Bilenkya, D. Lehnerc et al, Nucl. Phys. Proc. Suppl. B, **37**: 148, (1994)